

# Intraseasonal Variability of 2020 Temperature over Tanzania during the October-November-December (OND) Season

Godfrey Thomas Assenga<sup>1,2\*</sup>, Chabaga Chabaga<sup>2</sup>, Daudi Ndabagenga<sup>2</sup>, Daniel Gibson Mwangeni<sup>2</sup>

<sup>1</sup>Key Laboratory of Meteorological Disasters of Ministry of Education, Collaborative Innovation Center on Forecast and Evaluation of Meteorological Disasters, Nanjing University of Information Science and Technology, Nanjing, China

<sup>2</sup>Tanzania Meteorological Authority, Dodoma, Tanzania

Email: \*assengagt@gmail.com, met@meteo.go.tz

**How to cite this paper:** Assenga, G.T., Chabaga, C., Ndabagenga, D. and Mwangeni, D.G. (2025) Intraseasonal Variability of 2020 Temperature over Tanzania during the October-November-December (OND) Season. *Atmospheric and Climate Sciences*, 15, 126-146.

<https://doi.org/10.4236/acs.2025.151006>

**Received:** November 1, 2024

**Accepted:** January 5, 2025

**Published:** January 8, 2025

Copyright © 2025 by author(s) and Scientific Research Publishing Inc.

This work is licensed under the Creative Commons Attribution International License (CC BY 4.0).

<http://creativecommons.org/licenses/by/4.0/>



Open Access

## Abstract

Intraseasonal Oscillation (ISO) which is the eastward-propagating disturbance with a period of 10 - 60 days has been the topic of interest since its discovery by Madden-Julian in 1972. Many researchers have published their work on ISO, yet they all agree that there is no clear understanding of this matter. By using daily observed surface temperature (T2m), this study reveals the presence of significant biweekly ISO over Tanzania, a period shorter than the anticipated Madden-Julian Oscillation (MJO) period of 30 to 60 days. It also reveals significant changes in wind direction when comparing the cold phase to the warm phase, highlighting a distinct atmospheric circulation pattern associated with each phase. Furthermore, the analysis reveals the presence of MJO-like eastward movement of pressure systems in the Subtropical High region, which is associated with this variability. This study presents a new analysis by providing a detailed analysis of the intraseasonal variability (ISV) of temperature over Tanzania, focusing on understanding the 2020 spatial-temporal patterns within the October-November-December (OND) season that may play a role in weather forecasting, agricultural planning, climate adaptation, reducing heat-related illnesses and contributing to the international effort to refine climate models and predictability.

## Keywords

Intraseasonal Variability, Mascarene High, Biweekly Oscillation, OND Season

## 1. Introduction

Climate variability characterizes the natural fluctuation of climatic variables such

as temperature, wind patterns, precipitation, geopotential height, sea surface temperature and pressure systems which occur over different temporal and spatial scales. ISOs refers to periodic variations in the atmosphere that occur on time-scales of 10 to 90 days associated with the variations in deep convection, which can lead to changes in precipitation, cloud cover, temperature and winds [1]-[3]. Since the publication of the MJO by Madden and Julian in 1972 [3], many papers have been published on ISO with further findings and new contributions analyzing variability to the climate variables such as temperature and precipitation over different locations around the globe [4]-[10]. Related research has been conducted in other areas such as Mid-high latitudes [11]-[17]. In Tanzania, where a large portion of the population relies on rainfed agriculture, temperature fluctuations may affect crop yields, water availability, and food security [18]. It may also impact energy demand and supply, ecosystem and biodiversity management as well as climate and resilience, underscoring the crucial importance of studying the ISV of temperature over Tanzania.

Due to such effects, a number of studies have been carried out on the ISV of climate in East Africa and the world at large. In 2001, Mpeti & Jury observed that the most significant spectral energy for an area-averaged OLR index is concentrated in periods of 16 to 33 days, associating these Convective events over tropical East Africa with an influx of northeasterly Indian monsoon flow followed by increased westerlies from the Guinea/Congo region [19]. Also suggested that spectral peaks with periods greater than 30 days could be linked to the MJO and those in the 20 days range could be linked to tropical and mid-latitude waves. Also, Kijazi and Reason's analysis in 2005 revealed that spectral peaks of 10 - 20 days periods occurred 21% of the time, 20 to 30 day periods occurred 33% of the time, and >30 days (the MJO) were most prevalent at 46% [5]. This suggests that 54% of the period between 10 to 30 days falls under biweekly oscillation which is analyzed in this study. The weather over East Africa is largely influenced by the four high pressure systems located in the Subtropical high; Mascarene (MH), St. Hellena (SH), Azores and Arabian Ridge [20]-[22]. The anticyclonic circulation in the MH and its associated cross-equatorial winds are observed to play an important role in climate variability over the East African landmass [20] [22]-[24]. All these studies explained the link between MH and seasonal variability but not in the intraseasonal scale observed in this study. In Tanzania, the OND season, characterized by short rains, high variability, and prolonged dry spells, is significantly influenced by temperature variations. As a result, the ISV of temperature in Tanzania may significantly impact crop yields. Furthermore, Heat waves in Tanzania largely occur from October to March, as observed by Ndetto and Matzarakis [25] and Gyilbag *et al.* [26] making the OND season a preferable focus of our study.

Despite the extensive research on climate variability in East Africa and Tanzania, yet no specific study has focused on the ISV of temperature over Tanzania. The absence of ISV in temperature-focused research on Tanzania leaves unresolved questions about the presence of such oscillation. The main objective of this

study is to reveal the presence of ISV of temperature over Tanzania, analyzing time evolution and its associated weather system(s) by using 2020 OND season. It also aims at identifying the influence of the anomalous variability of the subtropical high on the ISV of temperature over Tanzania. This study presents a new analysis by providing a detailed periodic fluctuation of temperature over Tanzania during the OND season that may play a role in weather forecasting, agricultural planning, climate adaptation, reducing heat-related illnesses and contributing to the international effort to refine climate models and predictability. This research is organized as follows: Data and methodology in Section 2 provides a detailed description of the study area, including its location, topography, and climate, as well as the data description. It also outlines the statistical techniques employed, such as Lanczos filtering, bandpass filtering, composite spatial-temporal evolution, and composite analysis. Section 3 presents the results and their interpretation. Section 4 discusses the findings in the context of existing literature, and Section 5 concludes the study, highlighting key insights and implications.

## 2. Data and Methods

### 2.1. Study Area

Tanzania is a tropical country in East Africa located just south of the equator between latitudes  $0^{\circ}$  and  $12^{\circ}\text{S}$  and longitudes  $28^{\circ}\text{E}$  and  $42^{\circ}\text{E}$ . It also borders the Indian Ocean on its eastern side, and three great lakes: Lake Victoria in the North-western part, Lake Tanganyika aligning in the West and lake Nyasa in the South. It is also home to many rivers, hills, Serengeti plains and Ngorongoro crater. It is located to the east of the Congo Basin and the Congo Rainforest (**Figure 1**).

The country features complex topographical landscape including the highest point in Africa, Mount Kilimanjaro, which stands at 5895 meters.

Tanzania experiences two distinct climatic seasons which are the dry and wet seasons. The wet is classified into two distinct seasons: the long rains (Masika) from March to May (MAM) and the short rains (Vuli) from October to December (OND). Other months feature lower rainfall and generally cooler temperatures, particularly in the highlands and are classified as dry seasons. January and February are often the hottest months partly because of rainfall shortage while receiving high solar insolation over large part of Tanzania [5] [27] [28]. The diverse geography and topography shown in **Figure 1**, create distinct microclimates and climate patterns. Indian Ocean in the eastern part plays a crucial role in regulating the climate in the region. It is found that the warmer (cooler) than normal of East Africa-SST tend to influence the climate by suppressing (enhancing) OND rainfall in Tanzania [27]. Tanzania's climate variability is significantly influenced by Southern Hemisphere subtropical high-pressure systems, particularly the MH and the SH. The variability in these systems, along with the Indian Ocean Monsoon, Equatorial Low-Pressure System, East African Low-Level Jet (EALLJ), and South Indian Ocean cyclones, also impacts the region's westerly and easterly winds [20] [24] [28] [29].

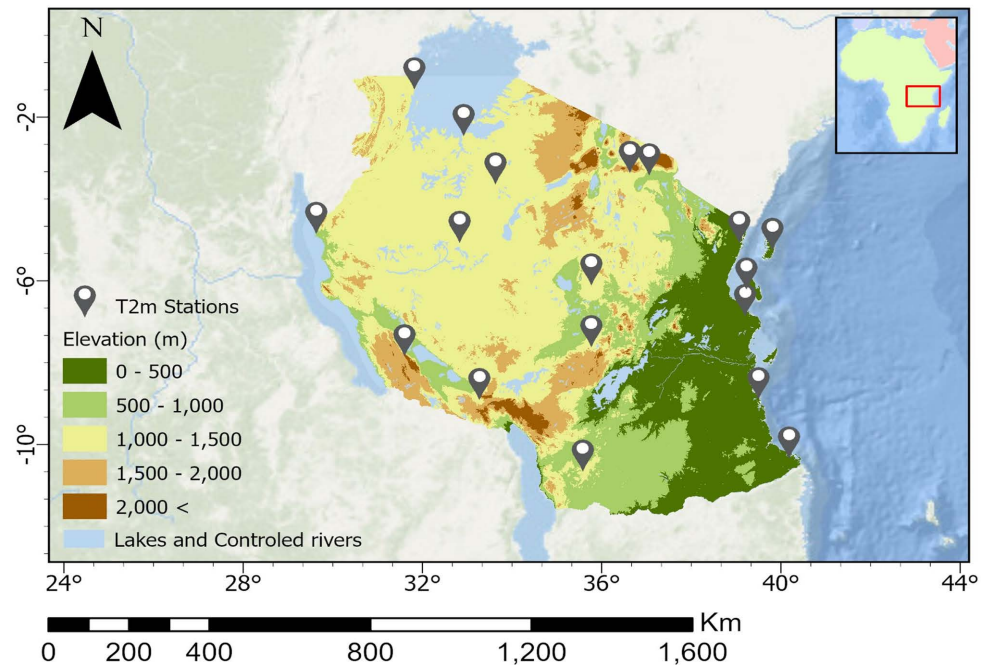


**Figure 1.** Map of Tanzania showing the elevation gradient with color shading, and the distribution of weather stations (marked by white dots with a gray background). The inset map shows Tanzania's location within Africa (red box). The elevation data illustrate topographical variations, relevant for understanding regional climatic and temperature differences.

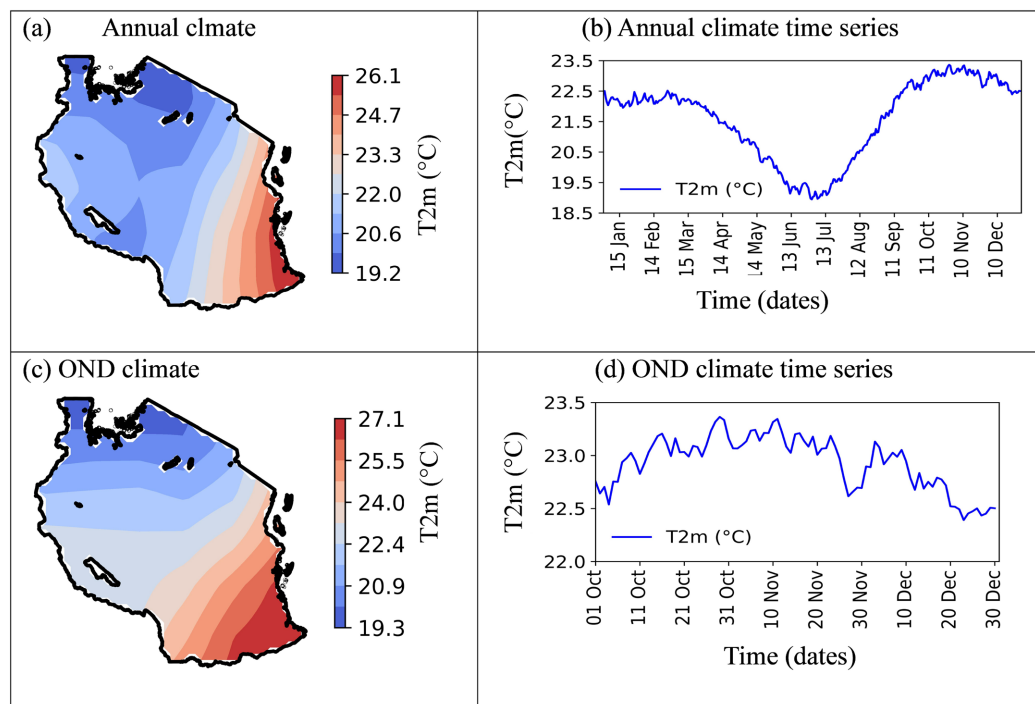


**Figure 2.** Illustration of the study area climate: (a) Annual T2m climatology across Tanzania, showing the average temperatures throughout the year. (b) Time series of T2m across Tanzania, highlighting temporal variability for Tanzania field mean T2m. (c) T2m climatology, emphasizing the seasonal temperature patterns during OND. (d) Time series of OND T2m climatology, illustrating the presence of periodic oscillations in the mean OND seasonal T2m.

The climatology map of Tanzania in **Figure 2(a)** shows that distribution of 2020 annual and OND T2m depends on the latitude, altitude, proximity to the Indian ocean and the presence of large water bodies such as lakes Victoria, Tanganyika and Nyasa. During OND season, the sun is on its way to the south, so southern parts gradually receive more solar insolation becoming warmer than the northern parts surrounding Lake Victoria (**Figure 2(c)**). Also, from the time series of the daily average T2m (**Figure 2(b)**), OND is relatively higher than other months. It can be observed that, Coastal areas are relatively warmer than the rest of the country due to the influence of Indian ocean temperature moderation. ISV of temperature along the coast is expected to be moderated by the influence of the sea surface temperature. **Figure 2(d)** shows the presence of oscillation in the OND season T2m climatic time series calculated from 40-year data (1979-2022).

## 2.2. Data

The station data consisting of daily Maximum and minimum temperature ( $^{\circ}\text{C}$ ) from 18 stations from years 2018-2022 were collected from Tanzania Meteorological Authority (TMA). For each station, the daily mean surface temperature (T2m) was calculated as the average of the maximum and minimum temperatures. The data were used as the primary data set for identification of temperature fluctuation period. The spatial distribution of the stations which are used in this study is illustrated in **Figure 1**. For further spatial-temporal analysis, it utilizes data from the NCEP/DOE Reanalysis 2 (R2) Project [30]. The dataset is available in NetCDF format and has temporal Coverage daily values derived from years 1979/01 to 2024/08, Spatial Coverage 2.5-degree latitude  $\times$  2.5-degree longitude global grid ( $144 \times 73$ ) 90N - 90S, 0E - 357.5E. It covers 17 pressure levels. Furthermore, this dataset has been applied by other researchers to examine intraseasonal variability of temperature over different regions hence it is appropriate for this study [5] [11] [19] [20] [22] [31]-[33].

## 2.3. Methodology

### 2.3.1. Temporal Analysis

Temporal analysis seeks to identify patterns such as trends, seasonality, and cyclic behavior in the observed data. This helps to describe the systematic components of the time series [34]. Cyclical components exist when data exhibit rises and falls that are not necessarily of fixed period. The average length of cycles is longer than the length of a seasonal pattern. In this study only one season during OND months is analyzed, which limits the influence of annual cycles in the time series. OND seasonal departures were calculated by subtracting the OND mean, highlighting fluctuations around the mean season which gives insight of the presence of ISV in the time series (e.g. biweekly, 30 to 60 days) [35]. The observed time series (seasonal departures) is smoothed by using two-sided averaging technique (centered moving average) shown in Equation (1). This helps to clearly view the seasonal patterns by removing the noises of higher frequencies [36].

$$\hat{T} = \frac{Y_{t-2} + Y_{t-1} + Y_t + Y_{t+1} + Y_{t+2}}{5} \quad (1)$$

where:  $\hat{T}$  is the smoothed value at  $t$ .

$Y_{t-2}$ ,  $Y_{t-1}$ ,  $Y_t$ ,  $Y_{t+1}$ ,  $Y_{t+2}$ , are values at times  $t - 2$ ,  $t - 1$ ,  $t$ ,  $t + 1$  and  $t + 2$  respectively.

Long-term trends are removed by fitting a polynomial regression model to the smoothed data to capture the remaining and then subtracted this polynomial trend from the smoothed data as shown in Equation (2).

$$X_t = a_0 + a_1t + a_2t^2 + a_3t^3 + e_t \quad (2)$$

where:  $X_t$  is the climatic variable (temperature)  $t$  is time,  $a_0$ ,  $a_1$ ,  $a_2$  and  $a_3$  are coefficients to be estimated and  $e$  is the error term.

### 2.3.2. Power Spectrum Analysis

The power spectrum method was used to transform time series discussed in previous section to a Period Domain. In this method, Fourier Transform was used to convert the time series data to a frequency (period) domain and compute the power spectrum. Dominant frequency (period) is identified by assessing the level of significance for different cycle periods and selecting the pattern which passes 95% confidence interval. Most studies of ISV of climate in Tanzania use pre-determined ISO indices such as MJO missing fast moving atmospheric patterns such as biweekly patterns. Power spectrum is a powerful method successfully used in many ISVs of climate researches [7] [12] [36] [37]. Unlike other techniques, such as simple trend analysis or autocorrelation, the power spectrum reveals how much variance in the data is associated with different frequency components. This is particularly useful for analyzing periodic or oscillatory behaviors, like intraseasonal climate variations, as it allows us to pinpoint specific periods of variability (e.g., biweekly or monthly cycles). Additionally, the power spectrum method is robust to noise, especially when combined with smoothing and confidence interval estimation, making it well-suited for detecting underlying patterns in complex, noisy climate data [38].

### 2.3.3. Band-Pass Filtering

Based on the results of the power spectrum analysis, a 10 - 25-day band-filtering was applied to the time series data using the Lanczos filtering method, as described by Yang and Li [11] to extract the biweekly component. Lanczos filtering is a digital signal processing technique that utilizes a mathematical approach based on the Lanczos kernel to reduce noise and extract meaningful signals from data. This method is particularly effective in mitigating Gibbs oscillations, which can distort the representation of signals when using traditional Fourier methods. The Lanczos filter is characterized by its ability to maintain a balance between low-frequency preservation and high-frequency rejection, making it a preferred choice for various applications in signal processing and data analysis [39].

This method is useful for isolating the dominant periodicity of interest from the spectral analysis results. It has been used successfully in many other studies,

including those by Yang and Li [40], Wen *et al.* [41] [42], Wang *et al.* [43], and Krishnamurti and Ardanuy [6]. It uses a linear relationship to transform the raw data sequence  $x_t$  into a filtered data sequence  $y_t$  as shown in Equation (3) and Equation (4).

$$y_t = \sum_{k=-n}^n w_k x_{t+k} \quad (3)$$

where;  $y_t$  is the bandpass filtered output at time  $t$ ,  $x_{t+k}$  is the input time series at time  $t+k$  and  $w_k$  are smoothed weights which for bandpass filtering, is written as

$$w_k = \left( \frac{\sin 2\pi f_{c2} k}{\pi k} - \frac{\sin 2\pi f_{c1} k}{\pi k} \right) \frac{\sin \pi k/n}{\pi k/n} \quad (4)$$

$$K = -n, \dots, 0, \dots$$

### 2.3.4. Composite Analysis

This method involved processing a gridded T2m dataset from NCEP/DOE Reanalysis 2 (R2) by using Python data analysis tool. A shapefile of Tanzania's administrative boundaries was used to clip the data to the study area. Lag phases were defined based on key dates (Table 1), and mean temperatures for each phase were calculated by averaging T2m data from selected dates. Warm events are considered as days with larger or equal to one standard deviation ( $>$  or  $=$  1std) and the average of the days with peak values are considered as day 0 (lag 0). Table 1 shows the peak days dates and their corresponding observed positive peak values. The results were visualized in a  $3 \times 3$  grid of subplots with contour plots and a diverging colormap to highlight the seasonal departures. By combining spatial and temporal dimensions, this methodology offers a powerful tool for understanding complex ISV of T2m in Tanzania, as demonstrated in the study by Bantzer and Wallace [44].

**Table 1.** Positive peak days and the corresponding peak values.

Date	Warm Peak Value
10 Oct 2020	1.53
25 Oct 2020	1.50
8 Nov 2020	1.38
25 Nov 2020	2.37

Filtered OND T2m, wind and geopotential height (hgt) maps are plotted in the interval of 2 days before and after day 0. Day  $-n$  and day  $n$  refer to  $n$  days before and after the peak temperature days (day 0), respectively. In the total 92 days during the OND, 2020, several peaks are chosen as the day 0 of the warm phase of ISV temperature cases in this study (Table 1).

Based on peak days average shown on Table 1, the composite time evolution of observed T2m (Figure 3) is used as the basis for the analysis of the composite time evolution maps using the gridded data. First T2m gridded data is filtered using a

band-pass filter to capture oscillations with a 10 to 25-day period for plotting a spatial maps time evolution then plots are analyzed to confirm whether the ISV of temperature prevails and link it with the atmospheric circulation patterns associated with it. The method has been used by several researchers to study ISV of climate [11] [15] [36] [37] [45].

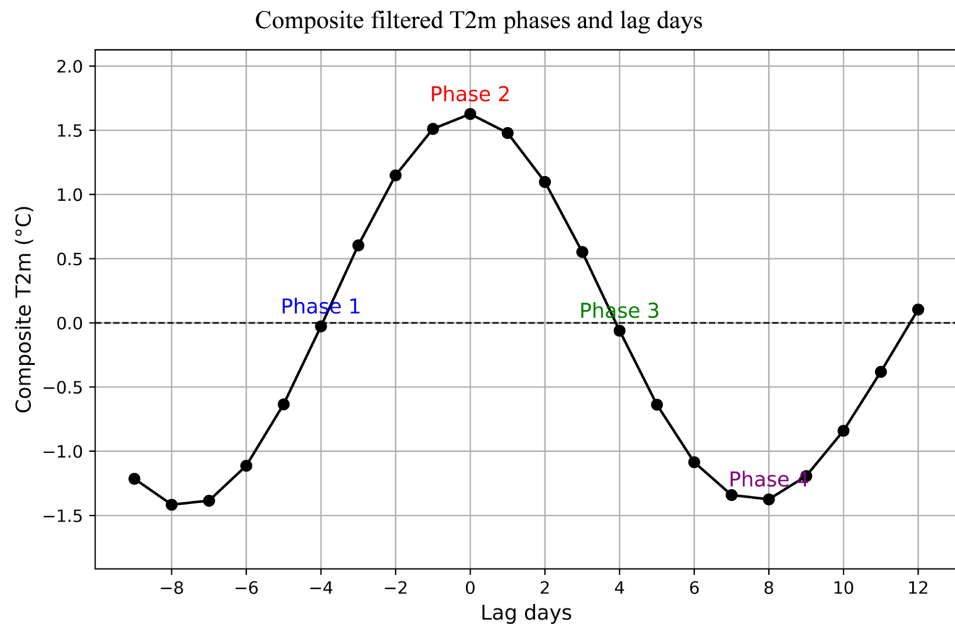


**Figure 3.** Evolutions of standardized composite 10 - 25-day filtered T2m (°C) (solid line) around average warm peak days in Tanzania, covering a period from 9 days before to 12 days after each peak. Dashed line at  $y = 0$  indicates the baseline. Phases are marked along the timeline, showing key stages in temperature evolution: Phase 1 (blue, -4 days), Phase 2 (red, peak day), Phase 3 (green, +4 days), and Phase 4 (purple, +8 days).

Negative peak events (**Table 2**) are also used to confirm the oscillation observed by using cold peak events. Overall, composite analysis is an effective tool for studying intraseasonal variability because it focuses on event-based analysis, enhances signal clarity, and provides insights into recurrent climate dynamics that may otherwise be obscured in raw, unaveraged data.

**Table 2.** Negative peak days and the corresponding peak values.

Date	Warm Peak Value
18 Oct 2020	-1.83
31 Nov 2020	-1.18
16 Nov 2020	-1.93
2 Nov 2020	-1.18

### 2.3.5. Statistical Significance Testing

To test the significance level of variability, Student's t-test method implemented by python analysis software is used to assess the statistical significance at 95%

confidence level ( $\alpha = 0.05$ ) according to the Equation (5).

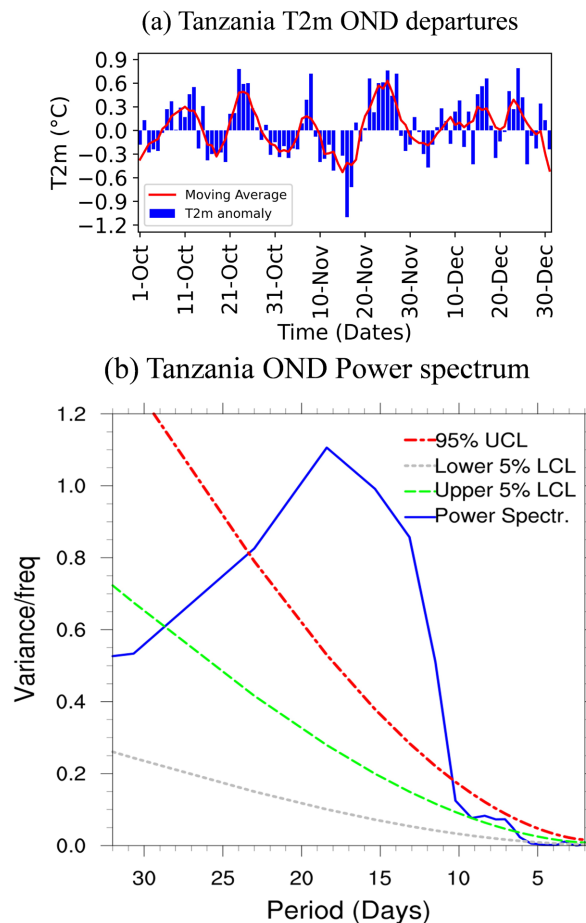
$$t = \frac{\bar{x}_1 - \bar{x}_2}{\sqrt{\frac{(n_1 - 1)S_1^2 + (n_2 - 1)S_2^2}{n_1 + n_2 - 2} \left( \frac{1}{n_1} + \frac{1}{n_2} \right)}} \quad (5)$$

where,  $n_1$  and  $n_2$  are sample sizes of the two groups,  $S_1^2$  and  $S_2^2$  are the sample variances of the two groups. This is used to test the significance of climate variability of the 10 - 25-day period filtered mean peak seasonal departures. The method has been successfully used by several researchers such as [24] [37] [45] [46].

### 3. Results

#### 3.1. Temporal Analysis of OND Season T2m

Analysis of the Time series of the Tanzania field mean shown in **Figure 4(a)** and the separate stations in **Figure 4(c)** shows a similar pattern of periodic oscillation. This implies that the field mean data is a good representation of individual T2m station data. This visualization highlights temperature deviations from the seasonal norm, providing insights into intraseasonal temperature changes across the OND season.



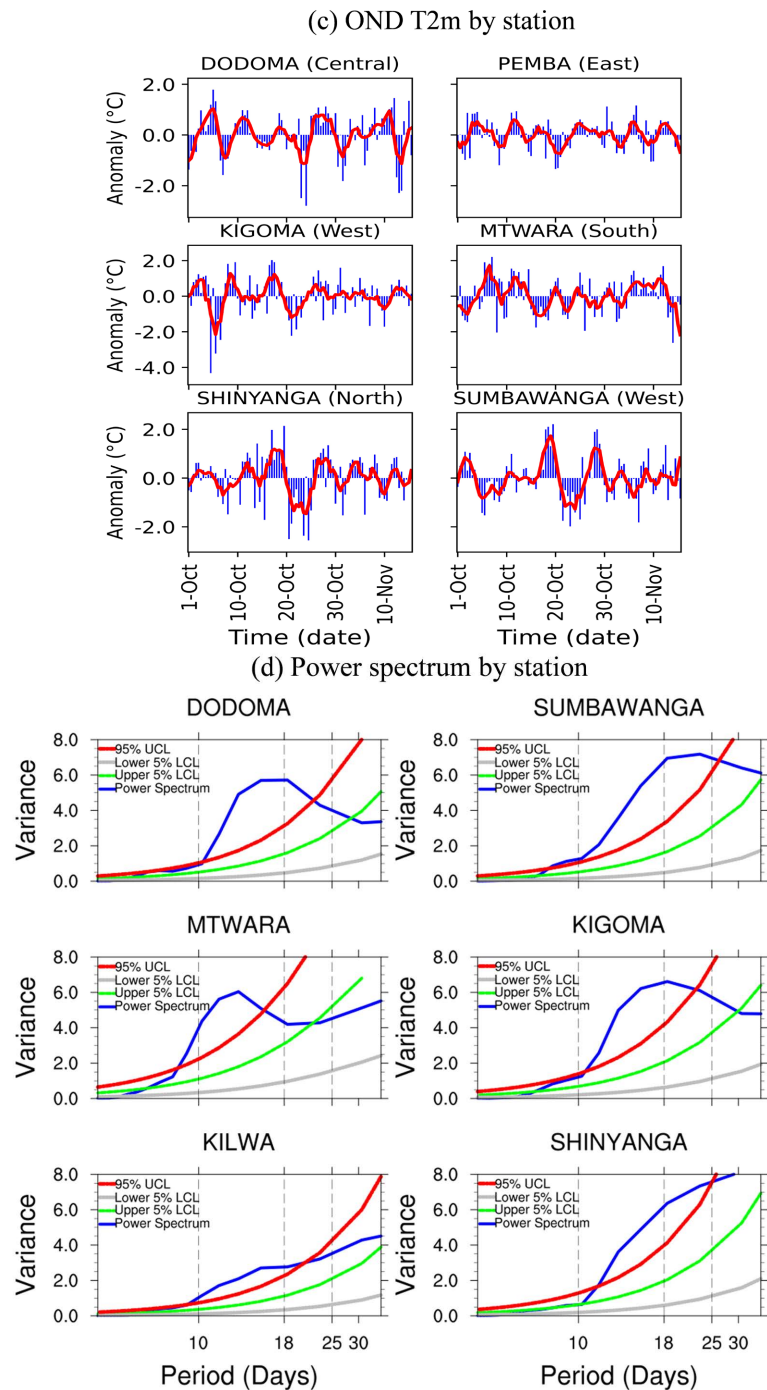


**Figure 4.** (a) Time series of daily T2m anomalies ( $^{\circ}\text{C}$ ) over Tanzania, showing seasonal deviations capturing day-to-day variability (blue bars) and a 5-day moving average to smooth short-term fluctuations (red line). (b) Power Spectrum of T2m anomalies during the OND Season over Tanzania to illustrate the power spectral density as a function of period (days) on a reverse x-axis, highlighting variance contributions across different time-scales. The blue line represents the power spectrum, while the green and gray lines indicate the 5% confidence interval boundaries, and the red line denotes the 95% upper confidence limit (UCL). Dashed vertical reference lines at 10-, 18-, and 25-day mark key intraseasonal periods, relevant to the study of oscillatory patterns in temperature variability. (c) as in (a) but for separate stations. (d) as in (b) but for each station in (c).

Through the power spectrum method, time series patterns observed in **Figure 4(a)** transformed into period domain as shown in **Figure 4(b)** and **Figure 4(d)**. The plot reveals that the power spectral density is concentrated within the 10- to 25-day period, which surpasses the 95% confidence interval, indicating significant variance contributions at these intraseasonal timescales

### 3.2. The Component of ISV of T2m

Based on the results of power spectrum analysis, the 10 - 25 days period component of the observation data is filtered and plotted as shown in **Figure 5**. Frequency band pass filtering with 95% confidence interval applied on temperature anomaly data based on lanczos filtering method shows the periodic patterns shown in **Figure 5**.

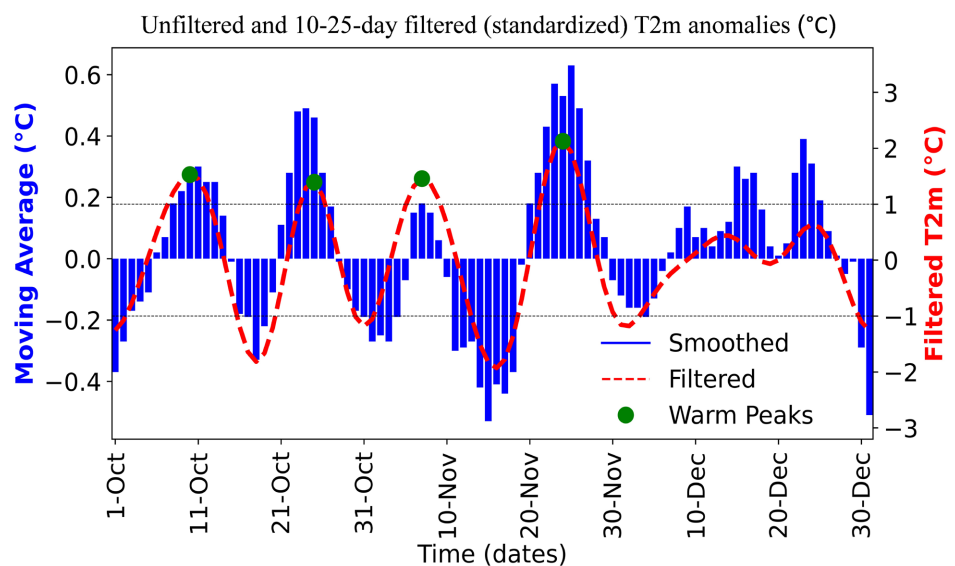


**Figure 5.** Standardized 10 - 25-day bandpass filtered signal of the OND season T2m ( $^{\circ}\text{C}$ ) departure series (red dashed line) alongside the raw 5-day moving average of T2m departures (blue bars). Warm peaks, identified as points where the bandpass-filtered signal exceeds +1 standard deviation, are marked with green circles. The dashed black lines at +1 and  $-1$  standard deviations denote the threshold for significant peaks, showing short-term temperature fluctuations within the 10 - 25-day period.

### 3.3. Spatial-Temporal Composite T2m Analysis over Tanzania

To analyze the T2m composite spatial-temporal evolution maps, **Figure 6** is plotted the same way as in **Figure 3** by using 10 - 25 days filtered NCEP II reanalysis gridded data. The aim is to analyze the T2m time evolution over the study area after every 2 days starting from 8 days before the peak, named as lag negative 8 ( $-8$  day) to 8 days after peak day, termed as lag positive 8 ( $+8$  day) to complete a cycle of 16 days. **Figure 6(a)** shows the composite time evolution plotted by using day 0 (lag 0) as the average warm peak date while other lag days are plotted at an interval of 2 days before and after peak day (lag 0). Likewise, **Figure 6(b)** illustrates the composite time evolution of the cold peak days. To test the significance of the

variability of the T2m over Tanzania, t-test analysis for warm and cold peaks are as illustrated in **Figure 6(c)** and **Figure 6(d)** respectively.

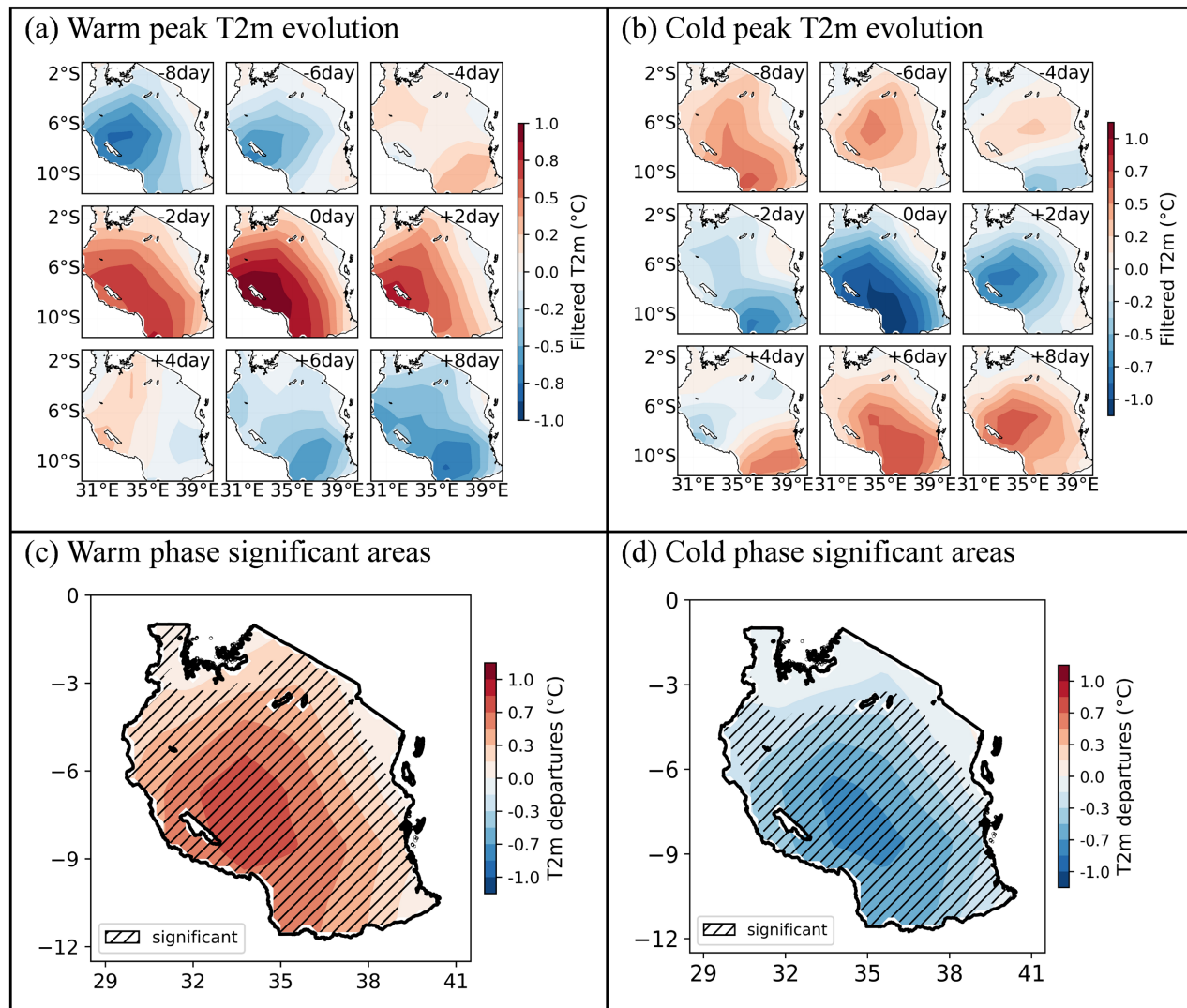


**Figure 6.** (a) Composite maps of 10 - 25-days filtered T2m anomalies ( $^{\circ}\text{C}$ ) over Tanzania, illustrating the spatial pattern of T2m variations across different lag days during the 2020 OND season. Each panel stands for lag days starting from 8 days before peak day (Lag 0) to 8 days after at an interval of 2 days, with lags displayed as days preceding ( $-$ ) or following ( $+$ ) lag 0. (b) as in (a) but plotted by using cold peaks. (c) Tanzania map highlighting deviations of warm peak days from the climatological mean T2m anomalies with hatching showing statistically significant areas ( $p < 0.05$ ). (d) as in (c) but for cold peak days.

### 3.4. The Evolution of Wind Circulation

To observe the atmospheric circulations associated with the illustrated T2m patterns over Tanzania, broader area composite time evolution is shown in **Figure 7**. The wind circulation is plotted from 10 - 25 days period of filtered wind data. The background shaded region represents filtered T2m over the broader area.

The region encircled in green shows the anomalous cyclonic flow while purple encircles the anomalous anticyclonic flow (**Figure 7**). **Figure 8** shows the two distinct phases which are the cold phase in **Figure 8(a)** and the warm phase

in **Figure 8(b)**. **Figure 8(c)** is the illustration of the significance test of the wind variability.

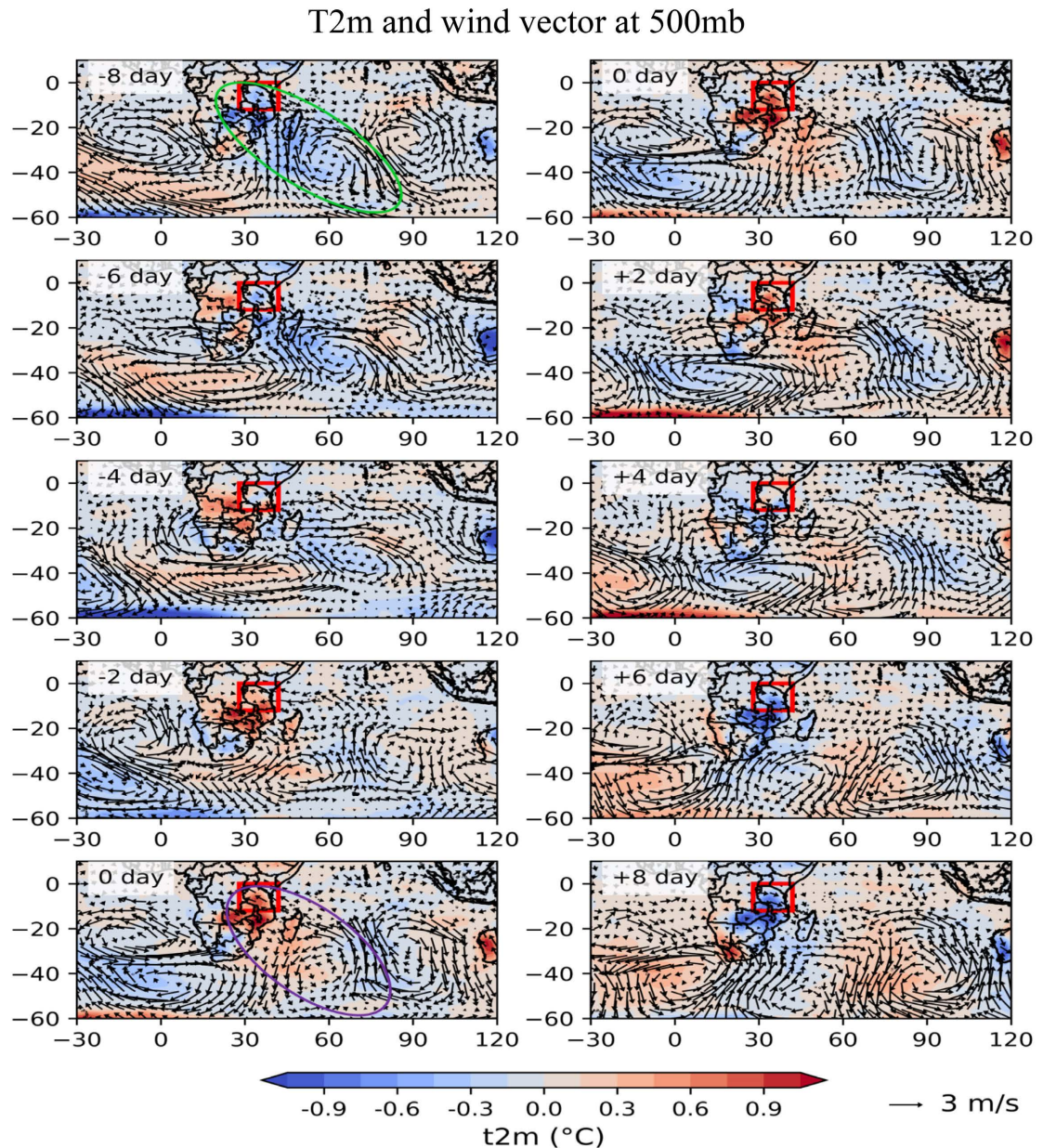


**Figure 7.** Temporal evolution of T2m (°C) and wind vectors (m/s) at 500 hPa from -8 to +8 lag days, shown at 2-day intervals during the OND season. Both T2m and wind vectors are values within the 10 - 25-day intraseasonal bandpass filter, averaged over the OND season. Lag -8 days highlights a region of anomalous cyclonic circulation (encircled in green), while lag 0 days shows anomalous anticyclonic circulation (encircled in purple) during peak phases.

The use of streamlines in plotting wind patterns shown in **Figure 8** facilitates the clear view of the link between the wind patterns over Tanzania and the atmospheric circulation systems based on the broader area specifically the subtropical high systems in the southern hemisphere.

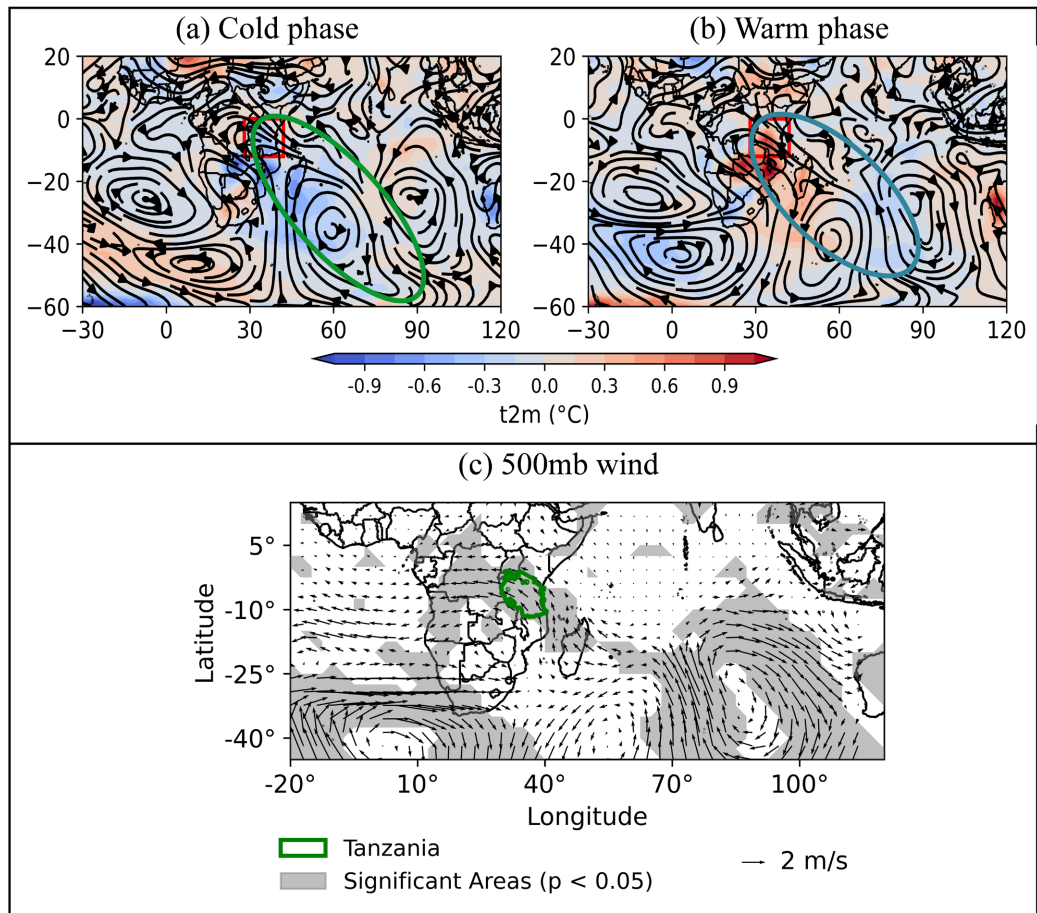


**Figure 8.** Composites of 10 - 25-day filtered spatial distribution of T2m anomalies and wind flow during peak phases over Tanzania, with the green boundary and red rectangle marking the study area. (a) Cold phase peaks of T2m anomalies, with contours indicating T2m ( $^{\circ}\text{C}$ ). Black streamlines depict the 500 hPa mean wind flow, while a green-encircled region highlights an anomalous cyclonic circulation. (b) Similar to (a) but for warm phase peaks, with purple-encircled regions indicating areas of anomalous anticyclonic flow. (c) Wind anomalies (m/s) at 500 hPa during peak phases, with grey shading highlighting areas where wind anomalies are statistically significant ( $p < 0.05$ ).

### 3.5. The Evolution of Geopotential Height

After analyzing wind systems, the link between the ISV of T2m over Tanzania and the variability of subtropical high-pressure systems in the Southern Hemisphere was established. The composite evolution of the 10 - 20 days period geopotential height, as shown in **Figure 9**, further illustrates this relationship.

The straight line with arrows shown in **Figure 9** illustrates the shifting of the geopotential height systems in the composite time evolution lag days. The red arrowed line represents the shifting of anomalous higher geopotential height, while the green line represents the shifting of low geopotential systems every 2 days.

## 4. Discussion

The temporal analysis (**Figure 4**) reveals a periodic oscillation in unfiltered T2m patterns, with **Figure 4(a)** and **Figure 4(c)** showing regular negative and positive

peaks corresponding to anomalous colder and warmer days. The power spectrum analysis confirms that, under the 95% confidence interval, spectral power peaks occur within a 10 - 25-day range, suggesting the presence of intraseasonal variability (ISV), particularly biweekly oscillations (ISO), in Tanzania. Tchinda [47] observed that ISV in Central Africa has two dominant frequency bands: the 10 - 25-day band and the 25 - 70-day band. The 10 - 25-day band aligns with the results of this study. These findings are significant for identifying dominant ISOs, which are essential for improving T2m forecasting in Tanzania and enhancing preparedness for temperature-related anomalies.

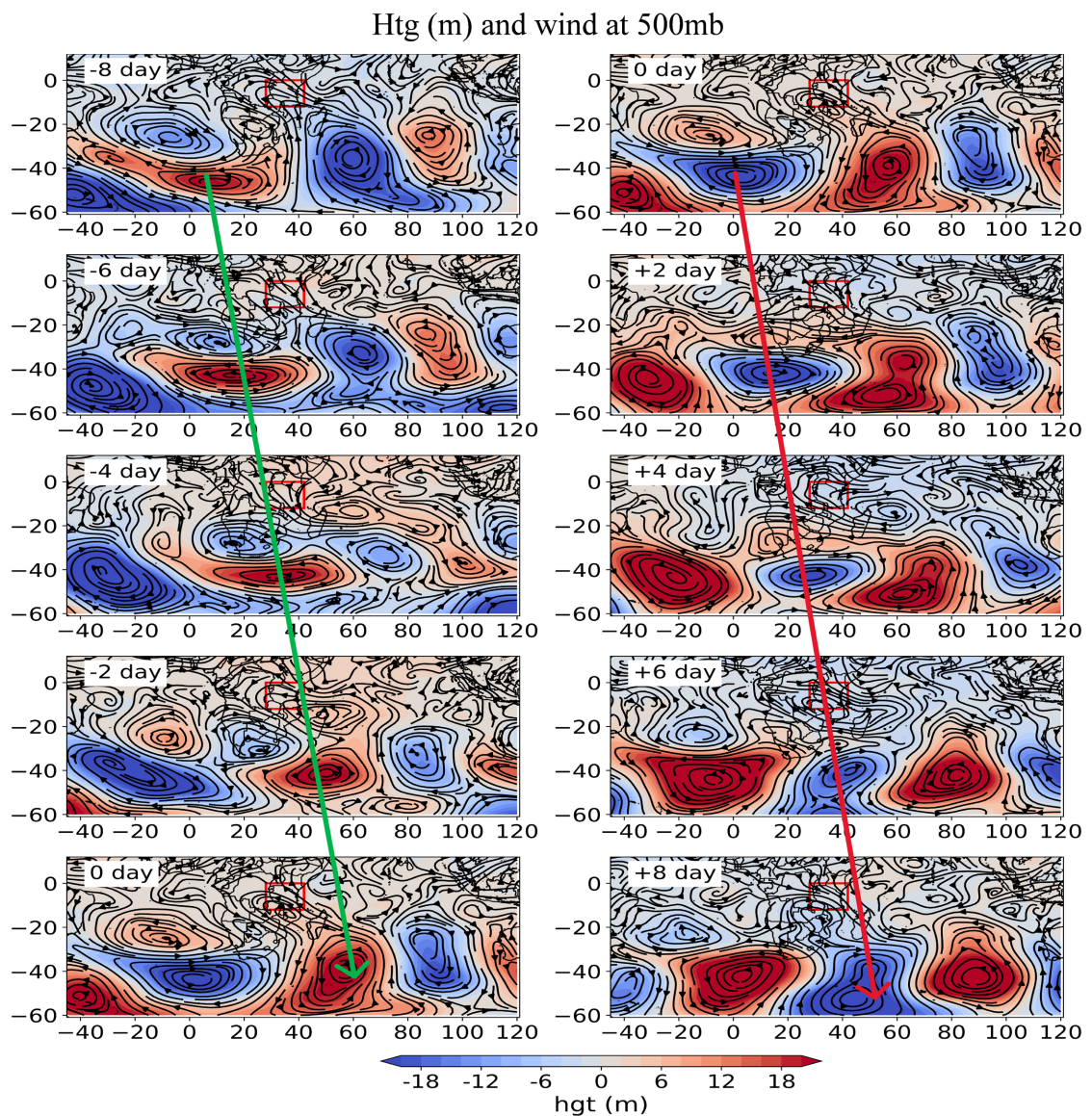


**Figure 9.** Composite time evolution of 10 - 25-days filtered geopotential height (m) shaded region overlaid by wind streamlines at 500 mb pressure level. The eastward movement of the high and low geopotential height (crossed by red and green arrows respectively) over the subtropical high, aligns with the classical intraseasonal oscillations discovered earlier such as MJO. The shift of this system appears to influence the wind system at 500 mb over Tanzania significantly during the cold and warm phases.

The bandpass filter analysis reveals four warm event peaks and four cold event peaks between October 1 and December 5, after which values fall below the defined threshold of one standard deviation, indicating an absence of discernible periodic temperature patterns. Among these, the two highest deviations from the seasonal mean occur on November 16 (negative) and November 25 (positive). The 10 - 25-day filtered T2m composite time evolution maps over Tanzania (**Figure 6**) reveal significant intraseasonal variability (ISV), marked by a warm anomaly peak at lag 0 and cold anomaly peaks at lags  $-8$  and  $+8$ . These findings suggest an intraseasonal oscillation (ISO) with a period of approximately 16 days, may significantly influence T2m distribution during the OND season of 2020. These oscillation patterns demonstrate significant predictive potential for identifying high-temperature days during the OND season, which is crucial for sectors like healthcare, agriculture, and communities exposed to direct sunlight. Kim *et al.* [48] highlights that understanding these oscillations enables improved predictions of heatwaves, informing public health strategies. By addressing this gap in seasonal temperature dynamics, the study underscores the importance of integrating predictive insights by adaptive strategies to enhance resilience, benefiting diverse sectors and vulnerable populations.

Wind analyses (**Figure 7**) further highlight the alternating high- and low-pressure systems, modulated by the Mascarene High (MH), which drive opposing wind patterns during warm and cold phases, underscoring the MH's role in Tanzania's seasonal climate dynamics. The analysis of the 10 - 25 days period geopotential height, shown in **Figure 9**, reveals an eastward movement of geopotential height with a biweekly scale in the subtropical high region, resembling MJO patterns. This movement, characterized by anomalous high- and low-pressure systems, may contribute to the intraseasonal variability (ISV) of temperature over Tanzania. During the cold phase, an anomalous cyclonic flow over the Mascarene High (MH) region is linked to northwesterly wind patterns across Tanzania. Conversely, during the warm phase, an anomalous anticyclonic flow over the MH drives southeasterly winds originating from the Indian Ocean, influencing Tanzania's temperature. Since the sun is in the Southern Hemisphere during this period, winds from the south are warmer compared to the cooler winds from the north. This has practical applications in agriculture, particularly in regions like Tanzania, where predicting rainfall and temperature fluctuations is crucial for optimizing crop yields. For instance, the study by Kumar and Sarthi [49] highlights how the ISV of climate influences tropical cyclones and rainfall patterns, underscoring the importance of understanding these oscillations to enhance climate prediction and agricultural planning. This highlights the need for further investigation into these dynamics to enhance climate resilience and disaster preparedness. By uncovering the significant role of subtropical pressure systems, such as the Mascarene High (MH), in Tanzania's ISV of climate, this study offers a fresh perspective on how southern hemisphere subtropical high systems influence regional weather patterns. These insights could play a crucial role in improving

climate adaptation strategies and forecasting models.

## 5. Conclusions

This research has provided valuable insights into the intraseasonal variability of temperature over Tanzania, revealing distinct patterns and fluctuations that are crucial for understanding the region's climate dynamics. Results from the power spectrum highlighted a dominant ISV of T2m for a 10 - 25 days period over Tanzania. Through a band-pass filter, four warm and cold peaks were identified and used in the composite time evolution.

The study revealed the presence of MJO-like anomalous high- and low-pressure systems propagating eastward within the subtropical high region of the Southern Hemisphere. It also demonstrated the connection between these oscillations and climate variability over Tanzania, particularly the ISV of T2m. Specifically, the findings highlight the role of the Mascarene High (MH) in regulating temperature patterns in Tanzania. Anomalous cyclonic flow over the MH region during the cold phase is associated with northwesterly wind patterns across Tanzania, while anomalous anticyclonic flow during the warm phase drives southeasterly winds from the Indian Ocean. These southeasterlies, occurring when the sun is in the Southern Hemisphere, bring warmer air compared to the cooler northwesterlies, thereby influencing Tanzania's temperature variability.

This suggests that the subtropical high region, especially the MH, contains valuable signals that can explain climate variability over Tanzania and contribute to weather prediction in the region. The findings establish a foundation for further research on the intraseasonal oscillation (ISO) in the subtropical high region of the Southern Hemisphere and its influence on climate variability across southern Africa, including East Africa.

Additionally, this study contributes to the growing body of knowledge on climate variability in East Africa and emphasizes the need for continued investigation into the Southern Hemisphere's complex climate systems. Future research could further enhance the understanding of temperature variability over Tanzania by examining how these variations manifest across multiple seasons and years to better understand the consistency and mechanisms linked to the observed eastward movement of the subtropical high system.

## Acknowledgements

We are deeply grateful to our supervisor, Prof. Shuangyan Yang, for her invaluable guidance and support throughout this research. We also sincerely thank Dr. Ladislaus Chang'a, Director General of the Tanzania Meteorological Authority, for providing access to the station-observed data crucial for this study. Special thanks go to Mr. Denish Madhushanka for his assistance with ArcGIS, which greatly contributed to the study area map, and to Mtupili Mtupili and Charles Ntigwaza for their insightful contributions and encouragement during this work. Their support was instrumental in the successful completion of this study.

## Conflicts of Interest

The authors declare no conflicts of interest regarding the publication of this paper.

## References

- [1] Wang, Y., Xiao, T., Dong, X., Li, Y., Huang, W. and Tan, J. (2022) Influence of 30-60 Days Intraseasonal Oscillation of East Asian Summer Monsoon on Precipitation in Southwest China. *Atmosphere*, **13**, Article 1222. <https://doi.org/10.3390/atmos13081222>
- [2] Wang, B. and Rui, H. (1990) Synoptic Climatology of Transient Tropical Intraseasonal Convection Anomalies: 1975-1985. *Meteorology and Atmospheric Physics*, **44**, 43-61. <https://doi.org/10.1007/bf01026810>
- [3] Madden, R.A. and Julian, P.R. (1994) Observations of the 40-50-Day Tropical Oscillation—A Review. *Monthly Weather Review*, **122**, 814-837. [https://doi.org/10.1175/1520-0493\(1994\)122<0814:ootdto>2.0.co;2](https://doi.org/10.1175/1520-0493(1994)122<0814:ootdto>2.0.co;2)
- [4] Borowiak, A., King, A. and Lane, T. (2023) The Link between the Madden-Julian Oscillation and Rainfall Trends in Northwest Australia. *Geophysical Research Letters*, **50**, e2022GL101799. <https://doi.org/10.1029/2022gl101799>
- [5] Kijazi, A.L. and Reason, C.J.C. (2005) Relationships between Intraseasonal Rainfall Variability of Coastal Tanzania and Enso. *Theoretical and Applied Climatology*, **82**, 153-176. <https://doi.org/10.1007/s00704-005-0129-0>
- [6] Krishnamurti, T.N. and Ardanuy, P. (1980) The 10 to 20-Day Westward Propagating Mode and “Breaks in the Monsoons”. *Tellus A: Dynamic Meteorology and Oceanography*, **32**, 15-26. <https://doi.org/10.3402/tellusa.v32i1.10476>
- [7] Liu, Y. and Yang, S. (2023) Characteristic Analysis of the 10-30-Day Intraseasonal Oscillation over Mid-High-Latitude Eurasia in Boreal Summer. *Atmosphere*, **14**, Article 1372. <https://doi.org/10.3390/atmos14091372>
- [8] Zhang, C., Gottschalck, J., Maloney, E.D., Moncrieff, M.W., Vitart, F., Waliser, D.E., *et al.* (2013) Cracking the MJO Nut. *Geophysical Research Letters*, **40**, 1223-1230. <https://doi.org/10.1002/grl.50244>
- [9] Zhang, Y., Li, T., Gao, J. and Wang, W. (2020) Origins of Quasi-Biweekly and Intraseasonal Oscillations over the South China Sea and Bay of Bengal and Scale Selection of Unstable Equatorial and Off-Equatorial Modes. *Journal of Meteorological Research*, **34**, 137-149. <https://doi.org/10.1007/s13351-020-9109-7>
- [10] Okello, O., Tan, G., Ongoma, V. and Nyandega, I. (2021) Influence of Convectively Coupled Equatorial Kelvin Waves on March-May Precipitation over East Africa. *Geographica Pannonica*, **25**, 24-34. <https://doi.org/10.5937/gp25-31132>
- [11] Yang, S. and Li, T. (2016) Intraseasonal Variability of Air Temperature over the Mid-High Latitude Eurasia in Boreal Winter. *Climate Dynamics*, **47**, 2155-2175. <https://doi.org/10.1007/s00382-015-2956-8>
- [12] Gao, Y., Hsu, P., Che, S., Yu, C. and Han, S. (2022) Origins of Intraseasonal Precipitation Variability over North China in the Rainy Season. *Journal of Climate*, **35**, 6219-6236. <https://doi.org/10.1175/jcli-d-21-0832.1>
- [13] Jiao, Y. and Wu, R. (2019) Propagation and Influence on Tropical Precipitation of Intraseasonal Variation over Mid-Latitude East Asia in Boreal Winter. *Atmospheric and Oceanic Science Letters*, **12**, 155-161. <https://doi.org/10.1080/16742834.2019.1586518>
- [14] Fan, L. and Yang, S. (2023) Impact of Westward-Propagating ISO over Mid-High-

- Latitude Eurasia on SSW during Boreal Winter. *Journal of Climate*, **36**, 6797-6816. <https://doi.org/10.1175/jcli-d-22-0843.1>
- [15] Frederiksen, J.S. and Lin, H. (2013) Tropical-Extratropical Interactions of Intraseasonal Oscillations. *Journal of the Atmospheric Sciences*, **70**, 3180-3197. <https://doi.org/10.1175/jas-d-12-0302.1>
- [16] Hoyos, C.D. and Webster, P.J. (2007) The Role of Intraseasonal Variability in the Nature of Asian Monsoon Precipitation. *Journal of Climate*, **20**, 4402-4424. <https://doi.org/10.1175/jcli4252.1>
- [17] Zhu, Z. and Li, T. (2017) Extended-Range Forecasting of Chinese Summer Surface Air Temperature and Heat Waves. *Climate Dynamics*, **50**, 2007-2021. <https://doi.org/10.1007/s00382-017-3733-7>
- [18] Waldock, C., Dornelas, M. and Bates, A.E. (2018) Temperature-driven Biodiversity Change: Disentangling Space and Time. *BioScience*, **68**, 873-884. <https://doi.org/10.1093/biosci/biy096>
- [19] Mpetta, E. and Jury, M. (2001) Intra-Seasonal Convective Structure and Evolution over Tropical East Africa. *Climate Research*, **17**, 83-92. <https://doi.org/10.3354/cr017083>
- [20] Manatsa, D., Morioka, Y., Behera, S.K., Matarira, C.H. and Yamagata, T. (2013) Impact of Mascarene High Variability on the East African 'Short Rains'. *Climate Dynamics*, **42**, 1259-1274. <https://doi.org/10.1007/s00382-013-1848-z>
- [21] Sun, L., Semazzi, F.H.M., Giorgi, F. and Ogallo, L. (1999) Application of the NCAR Regional Climate Model to Eastern Africa: 1. Simulation of the Short Rains of 1988. *Journal of Geophysical Research: Atmospheres*, **104**, 6529-6548. <https://doi.org/10.1029/1998jd200051>
- [22] Xing, L. and Ogou, K. (2015) Influence of Mascarene High and Indian Ocean Dipole on East African Extreme Weather Events. *Geographica Pannonica*, **19**, 64-72. <https://doi.org/10.5937/geopan1502064o>
- [23] Miyasaka, T. and Nakamura, H. (2010) Structure and Mechanisms of the Southern Hemisphere Summertime Subtropical Anticyclones. *Journal of Climate*, **23**, 2115-2130. <https://doi.org/10.1175/2009jcli3008.1>
- [24] Nkurunziza, I.F., Guirong, T., Ngarukiyimana, J.P. and Sindikubwabo, C. (2019) Influence of the Mascarene High on October-December Rainfall and their Associated Atmospheric Circulation Anomalies over Rwanda. *Journal of Environmental and Agricultural Sciences*, **20**, 1-20.
- [25] Ndetto, E.L. and Matzarakis, A. (2016) Assessment of Human Thermal Perception in the Hot-Humid Climate of Dar Es Salaam, Tanzania. *International Journal of Biometeorology*, **61**, 69-85. <https://doi.org/10.1007/s00484-016-1192-1>
- [26] Gyilbag, A., Amou, M., Tulcan, R.X.S., Zhang, L., Demelash, T. and Xu, Y. (2021) Characteristics of Enhanced Heatwaves over Tanzania and Scenario Projection in the 21st Century. *Atmosphere*, **12**, Article 1026. <https://doi.org/10.3390/atmos12081026>
- [27] Makula, E.K. and Zhou, B. (2022) Linkage of Tanzania Short Rain Variability to Sea Surface Temperature over the Southern Oceans. *Frontiers in Earth Science*, **10**, Article 922172. <https://doi.org/10.3389/feart.2022.922172>
- [28] Rowhani, P., Lobell, D.B., Linderman, M. and Ramankutty, N. (2011) Climate Variability and Crop Production in Tanzania. *Agricultural and Forest Meteorology*, **151**, 449-460. <https://doi.org/10.1016/j.agrformet.2010.12.002>
- [29] Finney, D.L., Marsham, J.H., Walker, D.P., Birch, C.E., Woodhams, B.J., Jackson, L.S., *et al.* (2019) The Effect of Westerlies on East African Rainfall and the Associated

- Role of Tropical Cyclones and the Madden-Julian Oscillation. *Quarterly Journal of the Royal Meteorological Society*, **146**, 647-664. <https://doi.org/10.1002/qj.3698>
- [30] NCEP (2000) NCEP/DOE Reanalysis 2 (R2). National Center for Atmospheric Research Computational and Information Systems Laboratory. <https://doi.org/10.5065/KVQZ-Y193>
- [31] Kalnay, E., Kanamitsu, M., Kistler, R., Collins, W., Deaven, D., Gandin, L., *et al.* (1996) The NCEP/NCAR 40-Year Reanalysis Project. *Bulletin of the American Meteorological Society*, **77**, 437-471. [https://doi.org/10.1175/1520-0477\(1996\)077<0437:tnyrp>2.0.co;2](https://doi.org/10.1175/1520-0477(1996)077<0437:tnyrp>2.0.co;2)
- [32] Hastenrath, S., Polzin, D. and Mutai, C. (2010) Diagnosing the Droughts and Floods in Equatorial East Africa during Boreal Autumn 2005-08. *Journal of Climate*, **23**, 813-817. <https://doi.org/10.1175/2009jcli3094.1>
- [33] Chan, R.Y., Vuille, M., Hardy, D.R. and Bradley, R.S. (2007) Intraseasonal Precipitation Variability on Kilimanjaro and the East African Region and Its Relationship to the Large-Scale Circulation. *Theoretical and Applied Climatology*, **93**, 149-165. <https://doi.org/10.1007/s00704-007-0338-9>
- [34] Buteikis, A. (2018) Time Series with Trend and Seasonality Components. 66. [http://web.vu.lt/mif/a.buteikis/wp-content/uploads/2019/03/Lecture\\_03\\_20190305.pdf](http://web.vu.lt/mif/a.buteikis/wp-content/uploads/2019/03/Lecture_03_20190305.pdf)
- [35] Yao, S., Sun, Q., Huang, Q. and Chu, P. (2016) The 10-30-Day Intraseasonal Variation of the East Asian Winter Monsoon: The Temperature Mode. *Dynamics of Atmospheres and Oceans*, **75**, 91-101. <https://doi.org/10.1016/j.dynatmoce.2016.07.001>
- [36] Gao, M., Yang, J., Wang, B., Zhou, S., Gong, D. and Kim, S. (2017) How Are Heat Waves over Yangtze River Valley Associated with Atmospheric Quasi-Biweekly Oscillation? *Climate Dynamics*, **51**, 4421-4437. <https://doi.org/10.1007/s00382-017-3526-z>
- [37] Wei, W., Li, W., Deng, Y. and Yang, S. (2018) Intraseasonal Variation of the Summer Rainfall over the Southeastern United States. *Climate Dynamics*, **53**, 1171-1183. <https://doi.org/10.1007/s00382-018-4345-6>
- [38] Landsberg, H.E., Mitchell, J.M. and Crutcher, H.L. (1959) Power Spectrum Analysis of Climatological Data for Woodstock College, Maryland. *Monthly Weather Review*, **87**, 283-298. [https://doi.org/10.1175/1520-0493\(1959\)087<0283:psaocd>2.0.co;2](https://doi.org/10.1175/1520-0493(1959)087<0283:psaocd>2.0.co;2)
- [39] Duchon, C.E. (1979) Lanczos Filtering in One and Two Dimensions. *Journal of Applied Meteorology*, **18**, 1016-1022. [https://doi.org/10.1175/1520-0450\(1979\)018<1016:lfloat>2.0.co;2](https://doi.org/10.1175/1520-0450(1979)018<1016:lfloat>2.0.co;2)
- [40] Yang, S. and Li, T. (2017) The Role of Intraseasonal Variability at Mid-High Latitudes in Regulating Pacific Blockings during Boreal Winter. *International Journal of Climatology*, **37**, 1248-1256. <https://doi.org/10.1002/joc.5080>
- [41] Wen, M., Yang, S., Higgins, W. and Zhang, R. (2011) Characteristics of the Dominant Modes of Atmospheric Quasi-Biweekly Oscillation over Tropical-Subtropical Americas. *Journal of Climate*, **24**, 3956-3970. <https://doi.org/10.1175/2011jcli3916.1>
- [42] Wen, M., Li, T., Zhang, R. and Qi, Y. (2010) Structure and Origin of the Quasi-Biweekly Oscillation over the Tropical Indian Ocean in Boreal Spring. *Journal of the Atmospheric Sciences*, **67**, 1965-1982. <https://doi.org/10.1175/2009jas3105.1>
- [43] Wang, L., Li, T., Zhou, T. and Rong, X. (2013) Origin of the Intraseasonal Variability over the North Pacific in Boreal Summer. *Journal of Climate*, **26**, 1211-1229. <https://doi.org/10.1175/jcli-d-11-00704.1>
- [44] Bantzer, C.H. and Wallace, J.M. (1996) Intraseasonal Variability in Tropical Mean

- Temperature and Precipitation and Their Relation to the Tropical 40-50 Day Oscillation. *Journal of the Atmospheric Sciences*, **53**, 3032-3045.  
[https://doi.org/10.1175/1520-0469\(1996\)053<3032:ivitmt>2.0.co;2](https://doi.org/10.1175/1520-0469(1996)053<3032:ivitmt>2.0.co;2)
- [45] Xue, F., Wang, H. and He, J. (2004) Interannual Variability of Mascarene High and Australian High and Their Influences on East Asian Summer Monsoon. *Journal of the Meteorological Society of Japan*, **82**, 1173-1186.  
<https://doi.org/10.2151/jmsj.2004.1173>
- [46] Zhang, W., Li, L. and Ren, J. (2022) Influence of Atmospheric 10-20 Day Low Frequency Oscillation on Regional Strong Cooling Events in the Winter of Northern China over the Past 40 Years. *Atmosphere*, **13**, Article 1406.  
<https://doi.org/10.3390/atmos13091406>
- [47] Tchinda, C.W., *et al.* (2023) The Influence of Intraseasonal Oscillations on Rainfall Variability over Central Africa: Case of the 25-70 Days Variability. *Scientific Reports*, **13**, Article No. 19842.
- [48] Kim, S., Kug, J. and Seo, K. (2020) Impacts of MJO on the Intraseasonal Temperature Variation in East Asia. *Journal of Climate*, **33**, 8903-8916.  
<https://doi.org/10.1175/jcli-d-20-0302.1>
- [49] Kumar, P. and Sarthi, P.P. (2021) Intraseasonal Variability of Indian Summer Monsoon Rainfall in CMIP6 Models Simulation. *Theoretical and Applied Climatology*, **145**, 687-702. <https://doi.org/10.1007/s00704-021-03661-6>